



A novel series of positive modulators of the AMPA receptor: Discovery and structure based hit-to-lead studies

Craig Jamieson^{a,*}, Stephanie Basten^b, Robert A. Campbell^a, Iain A. Cumming^a, Kevin J. Gillen^a, Jonathan Gillespie^a, Bert Kazemier^b, Michael Kiczun^a, Yvonne Lamont^a, Amanda J. Lyons^a, John K. F. Maclean^a, Elizabeth M. Moir^a, John A. Morrow^a, Marianthi Papakosta^a, Zoran Rankovic^a, Lynn Smith^a

^aMerck Research Laboratories, MSD, Motherwell, Lanarkshire ML1 5SH, UK

^bMerck Research Laboratories, MSD, PO Box 20, Oss 5340 BH, Netherlands

ARTICLE INFO

Article history:

Received 29 June 2010

Revised 30 July 2010

Accepted 31 July 2010

Available online 13 August 2010

Keywords:

AMPA receptor

Allosteric modulator

SBDD

Hit-to-lead

ABSTRACT

Starting from an HTS derived hit **1**, application of biostructural data facilitated rapid optimization to lead **22**, a novel AMPA receptor modulator. This is the first demonstration of how structure based drug design can be exploited in an optimization program for a glutamate receptor.

© 2010 Elsevier Ltd. All rights reserved.

The α -amino-3-hydroxy-5-methyl-4-isoxazole-propionic acid (AMPA) receptors are ionotropic glutamate receptors which are abundantly expressed in the central nervous system and are believed to facilitate the majority of fast excitatory amino acid neurotransmission.¹ The role of AMPA receptors appears to be critical to mediating synaptic plasticity and long-term potentiation (LTP), the use dependent enhancement in synaptic efficacy which is thought to encode various forms of learning and memory. AMPA receptor modulators have been shown to enhance LTP and are, therefore, under serious consideration as therapeutic agents for a range of neurological disorders including schizophrenia, Alzheimer's disease, Parkinson's disease and ADHD.^{2,3}

Subunits of the AMPA receptor are encoded by four distinct genes (GluA1–4), with each subunit comprising four domains: N-terminal, extracellular glutamate binding site (Ligand Binding domain, LBD), a transmembrane region and a C-terminal domain.⁴ In the last decade or so, significant advances have been made in studying the three-dimensional structure of the AMPA receptor with structures reported from a construct relating to the LBD (S1S2)⁵ and latterly the full-length receptor.⁶

Our research efforts were aimed at the identification of a novel series of AMPA receptor positive modulators which are of potential utility in the treatment of the kinds of neurological disorders delineated above. Following a high-throughput screening campaign using a functional assay with GluA1 overexpressed in HEK cells⁷, we identified compound **1** (Fig. 1) as a hit with confirmed activity from a well characterized solid sample. Compounds were inactive in the absence of glutamate, thus confirming their allosteric nature.

While compound **1** represented a tractable chemotype amenable to optimization and was deemed to have satisfactory potency ($pEC_{50} = 6.7$), further in vitro profiling revealed a number of deficiencies that required attention. Specifically, measured solubility was low (<1 mg/L) and there were attendant issues with microsomal stability (Rat/human intrinsic clearance, $Cl_i > 270 \mu\text{L}/\text{min}/\text{mg}$ protein).

From the outset of the program, we had access to biostructural data using the isolated S1S2 LBD GluA2 construct⁵ thus enabling an understanding of how our compounds interacted with the receptor.⁸ Figure 1 depicts hit compound **1** in complex with the S1S2 LBD GluA2 construct.⁹ Although our biological assay used the GluA1 receptor (wild type GluA2 is not permeable to calcium), in our hands X-ray crystallographic study of selected compounds in both GluA1 and GluA2 constructs showed the structures to be identical.¹⁰ Given that structures could be more expediently obtained with GluA2, we selected this construct for routine examination. Modulators of the AMPA receptor bind remotely to the

* Corresponding author. Address: Department of Pure & Applied Chemistry, University of Strathclyde, 295 Cathedral St., Glasgow G1 1XL, United Kingdom. Tel.: +44 141 548 4830; fax: +44 141 548 4822.

E-mail address: craig.jamieson@strath.ac.uk (C. Jamieson).

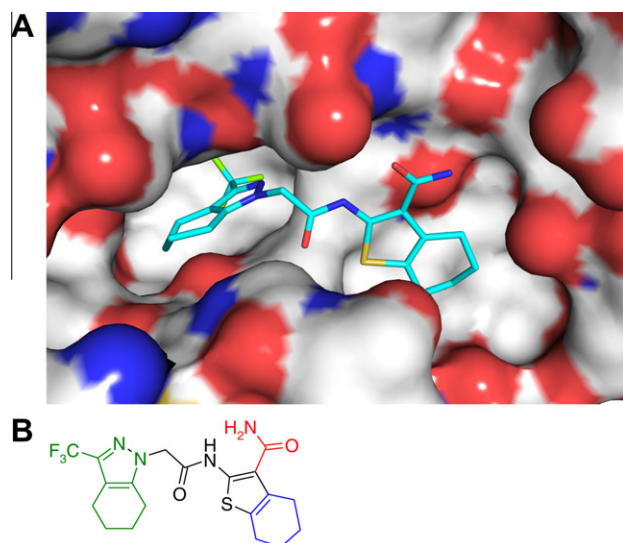


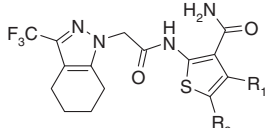
Figure 1. (A) Hit compound **1** in complex with S1S2 LBD of GluA2. Receptor surface is depicted, colored by atom type. Several residues have been omitted from this and subsequent figures for clarity. (B) Highlighted in green, red and blue are the three regions targeted.

orthosteric site and essentially stabilize a protein–protein interaction between the receptor subunits of each ligand binding domain.¹¹ Analysis of our X-ray data revealed that the interactions made with the receptor were primarily hydrophobic in nature, with key contacts made at the distal ends of the molecule (CF₃ moiety and tetrahydrobenzothiophene system). From consideration of the biostructural data, three principal regions of the molecule were targeted (shown in red, green and blue) in order to address the solubility and metabolism issues (Fig. 1).

Modification of the tetrahydrobenzothiophene portion (shown in blue, Fig. 1B) was expected to reduce lipophilicity and concomitantly improve potency and reduce propensity for hepatic metabolism. However, it was also anticipated that modulatory activity at the AMPA receptor may be negatively impacted by such changes.

Indeed, stripping back the fused cyclohexyl ring system to furnish for example compound **2** (Table 1) resulted in around a 30-fold reduction in potency, albeit with improvement observed in solubility (**2** showed kinetic solubility of 10 mg/L). Other truncated analogs (e.g., **3** and **4**) showed a similar reduction in potency without any improvement in solubility. Retention of the fused ring system with incorporation of a heteroatom was next explored in order to attenuate lipophilicity. Compound **5** displayed promising activity at the receptor but lacked any appreciable degree of

Table 1
Modifications to the tetrahydrobenzothiophene region



Compds	R ¹	R ²	pEC ₅₀ ^a
1		–(CH ₂) ₄ –	6.7
2	H	H	5.2
3	Me	Me	6.1
4	Et	Me	6.2
5		–CH ₂ –CH ₂ –O–CH ₂ –	6.7
6		–CH ₂ –CH ₂ –NH–CH ₂ –	5.3
7	CH ₂ OH	H	5.5

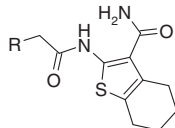
^a Values are means of two experiments performed in duplicate.

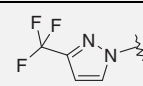
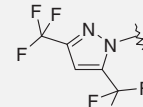
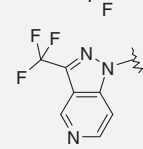
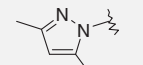
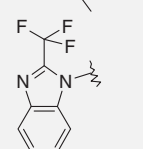
solubility (<1 mg/L) or metabolic stability (human and rat Cl_i >270 μL/min/mg protein). Insertion of a basic amine (**6**) or introduction of a pendant alcohol (**7**) led to a more than 10-fold reduction in potency.

In parallel, the contribution of the tetrahydroindazole system (shown in green, Fig. 1B) to AMPA modulatory activity was examined (Table 2). Deletion of the fused cyclohexyl ring (**8**) resulted in approximately a 30-fold reduction in potency presumably due to loss of a non-specific hydrophobic interaction. Activity could be partially restored by introduction of a 5-CF₃ substituent (**9**), however, again this was accompanied by low solubility and microsomal stability (solubility <1 mg/L, Cl_i (human) = 174 μL/min/mg protein, Cl_i (rat) = 200 μL/min/mg protein). A fully aromatic system (**10**) exhibited promising GluA1 activity, however, was again compromised by inadequate solubility (<1 mg/L) and less than optimal microsomal stability (Cl_i (human) = 153 L/min/mg protein, Cl_i (rat) = 91 μL/min/mg protein). As we expected from the biostructure of **1**, having a correctly orientated trifluoromethyl moiety is essential for activity. Replacement with a methyl (**11**) or altering the relative position (**12**) gave rise to inactive compounds.

The most effective means of meeting our optimization goals emerged from modification of the amide region of **1**. From consideration of the biostructural data, a hydrophilic pocket adjacent to the primary carboxamide motif (highlighted in red, Fig. 1B) could be accessed by suitably functionalized entities. We, therefore, focused our efforts in making modifications to this region. Initially, simple carboxamide derivatives were prepared (e.g., **13**, **14**, Table 3) which confirmed that substitution at this position would be tolerated. Encouraged by these results, we next prepared a number of more functionalized derivatives with pendant solubilizing groups. Evaluation of compound **15** in the GluA1 assay showed the compound had modest potency compared to our progenitor hit **1**. However, it was sufficiently potent to obtain biostructural data (Fig. 2) which revealed that contact with an Asp residue at the side of the hydrophilic pocket could be further optimized. We hypothesized

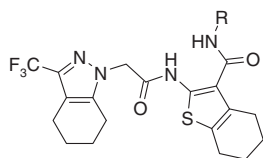
Table 2
Modifications to the tetrahydroindazole region



Compds	R	pEC ₅₀ ^a
8		5.3
9		5.8
10		6.4
11		<4.5
12		<4.5

^a Values are means of two experiments performed in duplicate.

Table 3
Modifications to the tetrahydrobenzothiophene region



Compds	R	pEC ₅₀ ^a
13	Et	6.5
14	cPropyl	6.2
15	$-CH_2CH_2NMe_2$	5.2
16	$-(CH_2)_3-NH_2$	6.4
17	$-CH_2CH_2NHMe$	5.7
18	$-(CH_2)_4-NH_2$	5.9
19	$-CH_2CH_2NH_2$	5.8
20	$-CH_2CH_2OH$	7.3
21	$-CH_2CH_2NHSO_2Me$	7.0

^a Values are means of two experiments performed in duplicate.

that either modification of the linker length, or removal of one or both of the *N,N*-dimethyl moieties could be beneficial to potency. In compound **15**, the binding mode of the tetrahydroindazole region was essentially identical to that observed with the progenitor compound (**1**).

These considerations led to the design of compound **16** which had comparable potency to the original hit. Other amine derivatives (e.g., **17–19**), although more potent than the progenitor **15**, were not as active at the receptor compared to compound **16**. The hydrophilic region proved to be relatively tolerant of other functional groups with alcohols typified by **20** and sulfonamide derivatives such as **21** displaying impressive potencies but in common with many other members of the series lacked solubility or microsomal stability.

In the series as a whole, compound **16** displayed the best balance of solubility (38 mg/L) and microsomal stability (human $Cl_i = 17 \mu\text{L}/\text{min}/\text{mg}$ protein, rat $Cl_i = 77 \mu\text{L}/\text{min}/\text{mg}$ protein). Permeability as measured by CaCo-2 was deemed to be low, however there was no indication of efflux ($A-B = 34 \text{ nm/s}$, $B-A = 55 \text{ nm/s}$). In vivo pharmacokinetics in Wistar rats (2 mg/kg iv, 10 mg/kg po) indicated moderate clearance and half-life in the iv leg ($Cl_p = 21 \text{ mL}/\text{min}/\text{kg}$, $T_{1/2} = 3.2 \text{ h}$, $V_{ss} = 3.8 \text{ L}/\text{kg}$), however, as anticipated from the CaCo-2 data, observed oral bioavailability was low (7.7%). Brain to plasma ratio was low (0.05) which was reasoned to be a function of both the number of hydrogen bond donors and rotatable bonds present in the molecule.

X-ray crystallographic data on the complex of **16** with the S1S2 LBD revealed the binding mode was as anticipated based on our

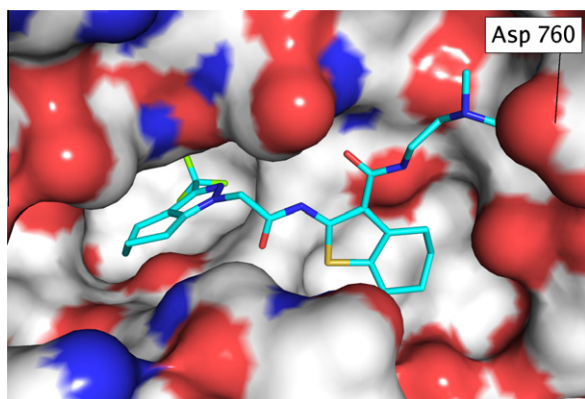


Figure 2. Biostructure of compound **15** in complex with the S1S2 LBD of GluA2.

observations from compound **15** (Fig. 3). The propylamine side chain was shown to project into the hydrophilic pocket as before, but now forming a salt-bridge with the side-chain of Asp 760. The biostructural data also suggested that conformationally constrained analogs of **16** could be accommodated in the hydrophilic region and this led to the design and synthesis of analogs **22–25** (Table 4) in an effort to improve brain penetration and oral bioavailability.

Comparing **22** and **23** shows a preference for the (*R*) stereochemistry on the pyrrolidine ring system. This was consistent with our expectations based on the conformation of the propylamine moiety required to facilitate the salt-bridge with Asp 760. The azetidines analogs **24** and **25** show similar potencies at GluA1 compared to **22**.

Further profiling of **22** indicated that the compound had both reasonable solubility (20 mg/L) and microsomal stability (human $Cl_i = 41 \mu\text{L}/\text{min}/\text{mg}$ protein, rat $Cl_i = 50 \mu\text{L}/\text{min}/\text{mg}$ protein). Assessment of permeability in the CaCo-2 assay suggested that absorption might still be an issue ($A-B = 19 \text{ nm/s}$, $B-A = 22 \text{ nm/s}$). In vivo pharmacokinetics in rat (2 mg/kg iv, 10 mg/kg po) indicated that **22** had low clearance and a reasonable half-life ($Cl_p = 2.3 \text{ mL}/\text{min}/\text{kg}$, $T_{1/2} = 3.8 \text{ h}$, $V_{ss} = 0.5 \text{ L}/\text{kg}$) and significantly improved brain exposure (brain:plasma ratio = 1.03). However, measured oral bioavailability was still low (3.8%) indicating that

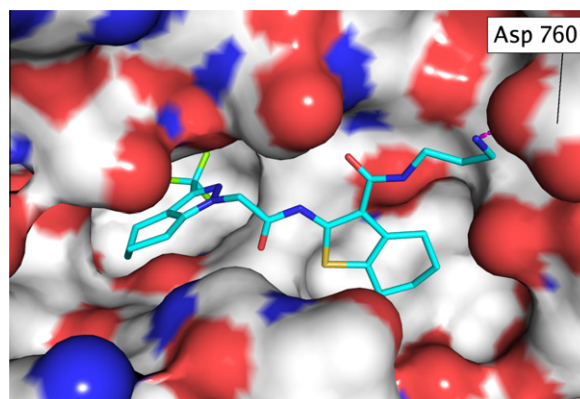
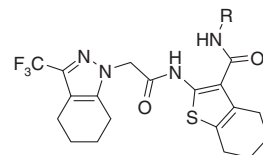


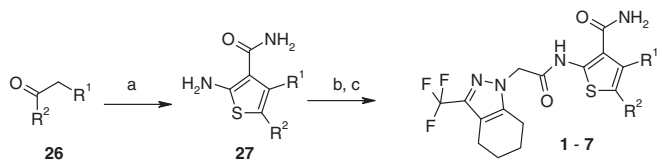
Figure 3. X-ray structure of **16** in complex with the S1S2 LBD of GluA2.

Table 4
Constrained analogs of compound **16**

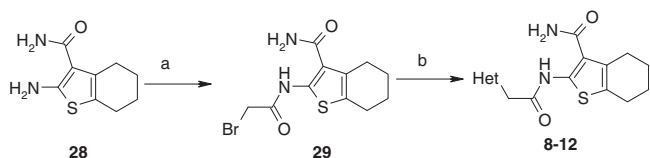


Compds	R	pEC ₅₀ ^a
22		6.6
23		5.8
24		6.5
25		6.2

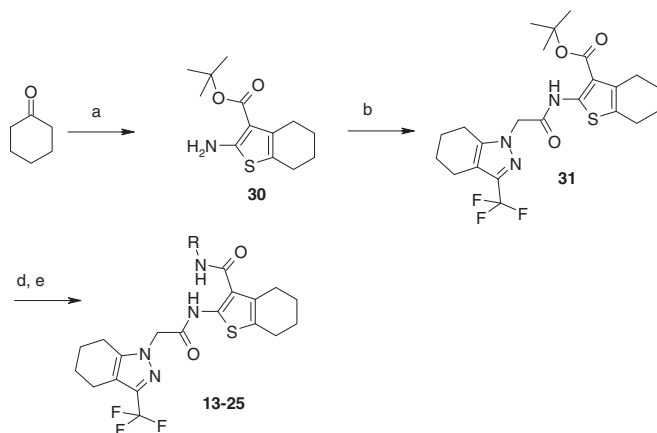
^a Values are means of two experiments performed in duplicate.



Scheme 1. Reagents and conditions: (a) sulfur, cyanoacetamide, diethylamine, EtOH, reflux 23–51%; (b) 3-(trifluoromethyl-4,5,6,7-tetrahydroindazol-1-yl)-acetic acid, PS-CDI, μ W, 120 °C, 10–53%; (c) TFA/ CH_2Cl_2 , rt, 23% (for **6**).



Scheme 2. Reagents and conditions: (a) bromoacetyl bromide, Et_3N , CH_2Cl_2 , rt, 94%; (b) azole derivative, NaH, DMF, 0 °C to rt, 14–49%.



Scheme 3. Reagents and conditions: (a) sulfur, *tert*-butylcyanoacetate, diethylamine, EtOH, reflux, 95%; (b) (3-(trifluoromethyl-4,5,6,7-tetrahydroindazol-1-yl)-acetic acid, HATU, DIEA, $\text{CH}_2\text{Cl}_2/\text{DMF}$, rt, 75%; (c) TFA/ CH_2Cl_2 , rt, quant.; (d) amine/Boc-diamine, HATU, DIEA, DMF, rt 10–70%; (e) TFA/ CH_2Cl_2 (for **16–19** and **22–25**), 15–40%.

conformational constraint alone was not sufficient to enhance this important parameter.

Synthetic approaches to the compounds discussed above are outlined in Schemes 1–3. Compounds **1–7** were prepared through a Gewald cyclization¹² to prepare the requisite tetrahydrobenzothiothiophene systems (**27**) followed by HATU mediated coupling to furnish compounds **1–7**.

Compounds **8–12** were synthesized in a two-step fashion from the available amino thiophene derivative **28** (Scheme 2). Acetylation with bromoacetyl bromide followed by alkylation of the appropriate azole derivative furnished the requisite target molecules in an expedient fashion.

Amide derivatives **13–25** were accessed as depicted in Scheme 3. Starting from cyclohexanone, Gewald cyclization furnished the aminothiophene ester **30**. Amide coupling provided intermediate **31** which was deprotected by acidolysis. Subsequent HATU mediated amide formation provided amides **13–15** and **20/21**. In the case of **16–19** and **22–25**, a Boc protected diamine derivative is employed in the coupling step with the desired amine unmasked in a final TFA deprotection step.

In summary, we have demonstrated how hit compound **1** was rapidly optimized to improve physicochemical parameters and metabolic stability resulting in compounds such as **16** and **22**. A central component of our expedient optimization trajectory has been the application of structure based drug design and is the first example of its use in a glutamate receptor system. Compounds such as **22** are useful tools in further elucidating the role of AMPA receptor modulators in debilitating neurological disorders such as Alzheimer's disease and Parkinson's. In the following paper, we describe how **22** can be further optimized to an orally bioavailable AMPA receptor modulator with promising *in vivo* activity.

References and notes

- Kew, J. N. C.; Kemp, J. A. *Psychopharmacology* **2005**, *179*, 4.
- Marenco, S.; Weinberger, D. R. *CNS Drugs* **2006**, *20*, 173.
- Zarate, J.; Manji, H. K. *Exp. Neurol.* **2008**, *211*, 7.
- Mayer, M. L.; Armstrong, N. *Annu. Rev. Physiol.* **2004**, *66*, 161.
- Armstrong, N.; Sun, Y.; Chen, G. Q.; Gouaux, E. *Nature* **1998**, *395*, 913.
- Sobolevsky, A. I.; Rosconi, M. P.; Gouaux, E. *Nature* **2009**, *462*, 745.
- HEK.GluR1(i) cells were maintained in DMEM supplemented with 10% fetal calf serum. Cells were maintained in DMEM supplemented with 10% non-essential amino acids and 150 $\mu\text{g}/\text{mL}$ hygromycin, at 37 °C/5% CO_2 . Twenty-four hour prior to the assay, the cells were harvested with trypsin and seeded onto Costar 96-well clear bottomed black plates at a density of 3.5×10^4 per well. Cells were loaded with 5 μM fluo3-AM in DMEM media in the absence of hygromycin and incubated at 37 °C/5% CO_2 for one h. After dye loading, the cells were washed once with 200 μl of low calcium solution (10 mM hepes, pH 7.4, 160 mM NaCl, 4.5 mM KCl, 2 mM CaCl_2 , 1 mM MgCl_2 , 10 mM glucose) containing 0.625 mM of probenecid to remove the dye. Then 200 μl of low calcium solution was added to each well. The FLEXstation added 50 μl of glutamate +/- test compound in high calcium solution (10 mM Hepes, pH 7.4, 160 mM NaCl, 4.5 mM KCl, 20 mM CaCl_2 , 1 mM MgCl_2 and 10 mM glucose) to each well and the ensuing response was monitored on FLEXstation.
- Crystals were grown as described in Ref. 5. Co-crystals were prepared by soaking test compound (100 mM) with crystals for 24 h prior to isolation and data collection. Coordinates and structure factors have been deposited in the Protein Data Bank for complexes of compounds **1** (3O28), **15** (3O29) and **16** (3O2A).
- The Pymol Molecular Graphics System (DeLano Scientific, Palo Alto, CA, 2002) was used to generate Figures 1–3.
- Maclean, J. K. F.; Kazemier, B. *J. Mol. Biol.*, in press.
- (a) Sun, Y.; Olson, R.; Horning, M.; Armstrong, N.; Mayer, M.; Gouaux, E. *Nature* **2002**, *417*, 245; (b) Ptak, C. P.; Ahmed, A. H.; Oswald, R. E. *Biochemistry* **2009**, *48*, 8594.
- Gewald, K.; Schinke, E.; Boettcher, H. *Chem. Ber.* **1966**, *99*, 94.